

# Perturbative Understanding of Non-Perturbative Processes and Quantumization versus Classicalization

Gia Dvali and Lukas Eisemann\*

*Arnold-Sommerfeld-Center, Ludwig-Maximilians-Universität,  
Theresienstraße 37, 80333 München, Germany and*

*Max-Planck-Institut für Physik, Föhringer Ring 6, 80805 München, Germany*

In some instances of study of quantum evolution of classical backgrounds it is considered inevitable to resort to non-perturbative methods at the price of treating the system semiclassically. We show that a fully quantum perturbative treatment, in which the background is resolved as a multi-particle state, recovers the semiclassical non-perturbative results and allows going beyond. We reproduce particle-creation by a classical field in a theory of two scalars as well as in scalar QED in terms of scattering processes of high multiplicity. The multi-particle treatment also gives a transparent picture of why a single-process transition from a classical to a quantum state, which we call quantumization, is exponentially suppressed, whereas the opposite process, classicalization, can take place swiftly if the microstate degeneracy of the classical state is high. An example is provided by the  $N$ -graviton portrait of a black hole: a black hole can form efficiently via a  $2 \rightarrow N$  classicalization process in the collision of high-energy particles but its quantumization via a decay  $N \rightarrow 2$  is exponentially suppressed.

## CONTENTS

I. Introduction	1
II. Example 1: $\phi^2\chi^2$	3
A. Coherent states and background fields	4
B. Quantum calculation	4
C. Semiclassical calculation	5
III. Example 2: Scalar QED	6
A. Quantum calculation	6
B. Semiclassical calculation	6
IV. Example 3: Scalar QED with massive photon	7
A. Semiclassical result	7
B. Quantum calculation	8
V. Parameter regimes	8
A. Semiclassical limit	8
B. Finite $g^2$	9
1. Effective potential	9
2. Diagrams with different $n$ -scaling	10
VI. Quantumization and classicalization	10
A. Quantumization	11
B. Classicalization	12
VII. Summary and outlook	13
Acknowledgments	14
References	14

## I. INTRODUCTION

It is common to classify quantum field theoretic phenomena into the sub-categories of *perturbative* and *non-perturbative* effects. A given effect is attributed to the non-perturbative category when its physical characteristics, such as a cross section or a transition rate, are not representable in the form of a perturbative power series in a relevant coupling constant.

A classic example is provided by the Hawking evaporation rate of a black hole. This rate is proportional to a negative power of the Newtonian gravitational coupling. It therefore creates the impression that the process is non-perturbative in Newton's constant. The same reasoning applies to many other examples of particle-creation in a background classical field.

In reality, in many instances, the underlying physics is fully perturbative in the coupling. This perturbativity becomes visible only upon the resolution of the classical background in form of a multi-particle state, such as a condensate, which may be realized in form of a number state or a coherent state. The corpuscular resolution makes transparent that a seeming non-perturbativity is the result of an interplay between the relevant coupling constant and the occupation number of quanta. This has been explicitly demonstrated for a number of systems.

For example, the theory of [1] offers a resolution of a black hole in form of a condensate (or a coherent state) of gravitons with occupation number  $N$ . This number is proportional to the inverse of the gravitational coupling. In this picture, Hawking evaporation is described as the depletion of the condensate due to re-scattering of constituent gravitons. The process is perturbative in Newton's coupling. The appearance of its negative power in the final expression of the evaporation rate is due to the Bose-enhancement of the process by the combinatorics of the occupation number  $N$ . Since  $N$  scales as the in-

\* lukas.eisemann@physik.lmu.de

verse of the Newtonian coupling, the rate also comes out to be inversely proportional to it. Hence the apparent non-perturbativity of the process.

In general, an understanding of non-perturbative mean-field effects as perturbative  $N$ -particle processes carries obvious advantages. In particular, it allows to go beyond the leading order approximation and to capture the  $1/N$ -corrections coming from quantum effects of the individual particles. Such effects are extremely important for properly accounting for the quantum back-reaction, which is due to particle-creation on a would-be classical background.

In certain cases this back reaction leads to a complete breakdown of the classical approximation. The concept was originally introduced within the framework of the black hole  $N$ -portrait [1], with the first explicit simulation of a prototype model conducted in [2], where the effect was referred to as *quantum breaking*.

Within the black hole  $N$ -portrait [1], it has been argued [3–6] that quantum breaking takes place at the latest by the time of half-decay.

Beyond black holes, the corpuscular approach to particle-creation has been applied to a number of other systems. In [5, 7–12] the classical de Sitter metric has been resolved as the coherent state of gravitons on the Minkowski vacuum. In particular, such a resolution is mandatory within the  $S$ -matrix formulation of gravity, since de Sitter cannot serve as a valid  $S$ -matrix vacuum [10]. In this picture, the Gibbons-Hawking particle-creation [13] is described as re-scattering of coherent state gravitons into all possible particle species. The back-reaction due to  $1/N$  effects leads to a gradual breakdown of the classical approximation. In particular, this is due to the generation of entanglement [5, 7, 8, 10, 11].

Likewise, an analogous corpuscular study of the decay of the coherently oscillating axion field was given in [14]. Some further studies on quantum breaking of coherent states using background field methods can be found in [15, 16]. For other aspects of the corpuscular resolution of de Sitter, cf. [17–19].

In all these examples, the non-perturbative semiclassical effect is recovered as the infinite- $N$  limit of the quantum picture.

The present paper represents a continuation of the above program but with some important novelties that allow to more cleanly extract the specific multi-particle effects in simple examples of basic importance. We study systems that represent the simplest prototype models describing the process of particle-creation by a background field. We do this both in the semiclassical approximation as well as in a fully quantum treatment. We show that the perturbative computation in the fundamental quantum theory captures the seemingly non-perturbative phenomena obtained in the semiclassical treatment of the same system.

In particular, we make a special focus on the regime when the energies of the produced quanta exceed the oscillation frequency of the background field. The non-

perturbative semiclassical analysis gives a very specific suppression of particle-creating instabilities. We show that the fully quantum treatment, perturbative in coupling  $g^2$ , reproduces these semiclassical results in large- $N$ .

To be more precise, this correspondence becomes exact in the following double-scaling limit,

$$g^2 \rightarrow 0, \quad \frac{N}{Vm^3} \rightarrow \infty, \quad g^2 \frac{N}{Vm^3} = \text{fixed}, \quad (1)$$

where  $m$  is the mass of the particles composing the would-be classical field and  $V$  is the volume. However, for finite values of the coupling  $g^2$  and the particle number density  $N/V$ , the fully quantum perturbative analysis allows to go beyond the semiclassical approximation and capture effects that are higher order in  $1/N$ .

We consider three examples. In the first example, the quanta of a scalar field  $\chi$  are created in the background of an oscillating classical scalar field  $\phi$ . The coupling between the two fields is  $g^2$ . At the level of semiclassical analysis, in which  $\phi$  is treated classically, such systems have been widely considered and have many applications, e.g., for reheating after inflation [20]. In this approximation, the creation of  $\chi$ -quanta is accounted for by certain instabilities in the background mode equation. It is usually said that these effects are non-perturbative. This may create the false impression that they cannot be captured by a perturbative analysis. We show that this is not the case.

We achieve this by giving a fully quantum resolution of the system. Namely, we represent the classical  $\phi$  field as a quantum state of high occupation number  $N$ . In this language, the particle-creation can be understood as a scattering process in which a number  $n$  of  $\phi$ -quanta is converted into a pair of  $\chi$ s. We show that the perturbative treatment fully captures the seemingly non-perturbative effect obtained in the semiclassical theory.

In two further examples, we generalize the effect to systems with gauge symmetry. One of these examples considers production of photons by a time-dependent charged scalar field. Here, too, the semiclassical picture is fully reproduced by perturbative quantum re-scattering of the charged constituent quanta of the condensate.

The final example is concerned with the inverted situation, i.e., production of a pair of scalar electrons in an oscillating electric field. In quantum language we describe this process as the creation of a particle-antiparticle pair in the annihilation of many photons. These photons represent the quantum constituents of the background electric field.

Our study has implications for fundamental questions regarding classical-to-quantum transitions and vice versa. In particular, it shines light on the question how fast a classical system can transit to a quantum state in which the classical approximation ceases to be valid. In [2], the timescale of such a breakdown was called the *quantum break-time*, which we denote by  $t_Q$ . The physically relevant timescale to which it must be compared

is the characteristic inverse frequency of the constituents of the classical state. In our examples, this is the frequency of the coherent oscillations of the classical field or a condensate. In the case of the  $N$ -portraits of black holes [1] and of de Sitter [1, 5], the basic frequency of the constituent gravitons is given by the inverse of the classical curvature radius.

The study performed in [2] shows that in a classically unstable system (i.e., a system with Lyapunov instability),  $t_Q$  can scale logarithmically in the number  $N$  of the system's constituents. Thus, such a system can quantum break swiftly.

On the other hand, in generic classically-stable or stationary systems, the quantum break-time was argued to be macroscopic in  $N$  [5, 7, 8]. In such systems the transition to a quantum state is gradual and quantum breaking is a cumulative effect of a large number of elementary processes, each with participation of a small number of quanta. In particular, this was argued to be the case for black holes [1, 3–6], as well as for de Sitter [5, 7–11].

In contrast, the quantum breaking driven by single-process transitions, with participation of order  $N$  constituents, are expected to be highly suppressed. Our analysis contributes to this understanding substantially. Due to the physical importance of this regime, we shall introduce a special term for such a process and refer to it as *quantumization*.

The flip side of the coin is the process called *classicalization* [21]. It represents a process of an inverse transition from a quantum state of few (say, two) energetic quanta into a classical state of soft quanta of high occupation number  $N$  [22–26]. Thus, the basis for both processes, quantumization as well as classicalization, is the  $S$ -matrix element between 2-particle and  $N$ -particle number eigenstates.

On very general physics grounds one can argue [26] that the square of such a matrix element is limited from above by an exponentially small factor  $e^{-N}$ . This has been confirmed by explicit computations, for example, by the computation of  $2 \rightarrow N$  graviton scattering [24]. In fact, for the systems we consider in the present paper, in certain regimes we shall obtain an even stronger suppression.

Although the basic matrix elements for quantumization and classicalization processes are the same, their physical manifestations are very different. The significance of  $2 \rightarrow N$  versus  $N \rightarrow 2$  has already been appreciated within the black hole  $N$ -portrait [1] and is generic for any classicalizing theory [25, 26].

The reason is the exponential difference between the degeneracies of  $N$ -particle and 2-particle microstates connected by one and the same matrix element. Correspondingly, it makes all the difference whether  $N$  appears in the initial or the final state of the process. The classicalization processes,  $2 \rightarrow N$ , can take place with order-one probability provided the  $N$ -particle classical state has a sufficient microstate entropy [1, 25, 26]. Such states in [26] were called “saturons”, as their entropy is close to

saturation the upper bound imposed by unitarity.

In contrast, the quantumization processes,  $N \rightarrow 2$ , are always exponentially suppressed. This is due to the fact that a valid 2-particle state has insufficient degeneracy for compensating the exponentially suppressed  $S$ -matrix element.

A good example of the difference between classicalization and quantumization processes is provided by black hole formation and decay as described by its  $N$ -portrait [1]. Since in this theory a black hole is a state of  $N$  soft gravitons, its formation in a collision of two high energy particles represents a process of classicalization,  $2 \rightarrow N$ .

The computation of the  $2 \rightarrow N$  graviton process [24, 27] shows that the probability of formation for each microstate is  $e^{-N}$ . However the suppression is compensated by the microstate degeneracy factor  $e^N$ . In other words, the black hole has sufficient degeneracy for compensating the exponentially suppressed matrix element, i.e., it is a saturon [26].

In contrast, a decay of a black hole into two very energetic quanta, represents a quantumization process of the type  $N \rightarrow 2$ . The microstate degeneracy of the final 2 particle state is negligible as compared to the exponential suppression. This explains the well-known property of black holes that, while they can form very fast, they always decay very slowly. Due to suppressed quantumization the decay happens via gradual emission of quanta through Hawking radiation, as opposed to an explosive decay into a few particles.

Also, one more physical consequence of the suppressed quantumization is an inability of the classical system to evolve into a highly entangled quantum state via a single-step process.

The examples studied in the present paper make these generic features of fundamental importance very transparent.

## II. EXAMPLE 1: $\phi^2\chi^2$

For the first example, we consider the model

$$L = \frac{1}{2}\partial_\mu\phi\partial^\mu\phi - \frac{1}{2}m^2\phi^2 + \frac{1}{2}\partial_\mu\chi\partial^\mu\chi - \frac{1}{2}m_\chi^2\chi^2 - g^2\phi^2\chi^2. \quad (2)$$

In a semiclassical treatment, an initial  $\phi$ -condensate is described by the classical solution

$$\phi_B(t) = \phi_0 \cos(mt), \quad \chi_B = 0, \quad (3)$$

and the fluctuations around the background (3) are quantized:

$$\hat{\phi} = \phi_B + \hat{\delta}\phi, \quad \hat{\chi} = \hat{\delta}\chi. \quad (4)$$

The initial state we would like to consider is then

$$|t_0\rangle = |0\rangle_{\delta\phi}|0\rangle_\chi. \quad (5)$$

The background alters the propagation of fluctuations to allow for particle-creation out of the vacuum, for example

$$0 \rightarrow 2\chi. \quad (6)$$

By contrast, in a fully quantum treatment, the condensate is described by an initial state

$$|t_0\rangle = |N\rangle_\phi |0\rangle_\chi, \quad (7)$$

where  $|N\rangle_\phi$  denotes a state of  $\phi$ -quanta in the mode of vanishing 3-momentum,  $\mathbf{p} = 0$ , in a superposition centered around the mean occupation  $N$ . This could, in particular, be a coherent state or simply a number state, and the consideration in the limit (1) is independent of the choice. For definiteness, we are going to assume a number state for now. The quantum processes giving rise to creation of a pair of  $\chi$ s are then

$$N\phi \rightarrow (N - n)\phi + 2\chi. \quad (8)$$

Here, the final  $\phi$ s are understood to be also in the  $\mathbf{p} = 0$  mode. Of course there are also processes involving scattered  $\phi$ s. As compared to (8), these are however suppressed by extra powers of the coupling  $g^2$  and vanish in the limit (1). Such suppression is not accompanying diagrams with only forward-scattered  $\phi$ s, but those contribute to the same process (8) (see also sec. V). In the absence of an elementary self-interaction of  $\phi$ , and in the regime of negligible Coleman-Weinberg correction to the potential, the energetics of the condensate are well approximated by

$$\frac{N}{V} = \frac{m\phi_0^2}{2}. \quad (9)$$

This relates the quantum and classical parameters. Thus, in semiclassical terms, the limit (1) reads

$$g^2 \rightarrow 0, \quad \frac{\phi_0^2}{m^2} \rightarrow \infty, \quad g^2 \frac{\phi_0^2}{m^2} = \text{fixed}. \quad (10)$$

In the following, we are going to compare the quantum-perturbative and semiclassical-non-perturbative prediction for creation of  $\chi$ -pairs with momenta  $k \equiv |\mathbf{k}|$  corresponding to

$$n \gg \frac{g\phi_0}{m}. \quad (11)$$

### A. Coherent states and background fields

Before going to the calculations of the rate, we would like to recall a general correspondence between calculations in a semiclassical approximation and a fully quantum one that involves coherent states [28]. In the notation of the example introduced above, consider a coherent state  $|c\rangle$  with the property  $\langle c|\hat{\phi}(t)|c\rangle = \phi_B(t)$  and  $\langle c|\hat{\chi}(t)|c\rangle = \chi_B(t)$ , where  $\hat{\phi}(t)$  and  $\hat{\chi}(t)$  are evolving according to the free Hamiltonian. For such a state, the

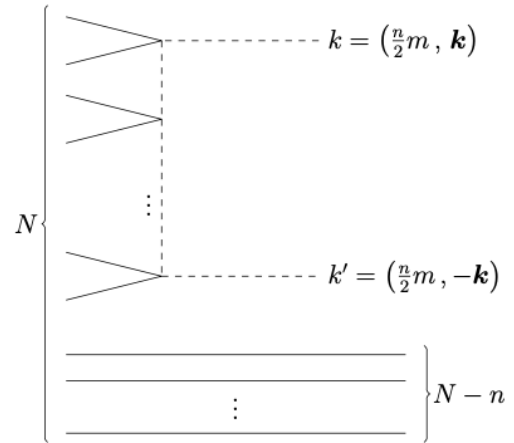


FIG. 1. Diagrammatic representation of the leading order terms in perturbation theory contributing to the amplitude of the process (8).

S-matrix operator in the presence of a background field agrees with the one of the fully quantum theory between  $|c\rangle$ ,

$$\langle c, B|\hat{S}|c, A\rangle_{\phi, \chi} = \langle B|\hat{S}[\phi_B, \chi_B]|A\rangle_{\delta\phi, \delta\chi}, \quad (12)$$

where the states  $|A\rangle$  and  $|B\rangle$  denote arbitrary number eigenstates of modes that are not contained in the background. As we shall see, the convergence of a perturbation series in the field strength depends also on the multiplicity  $n$  of the process under consideration. For the condensate decay (6) and (8) in question, identity (12) means that in the perturbative regime we have to find agreement of the perturbative fully quantum and non-perturbative semiclassical creation rates with any differences arising from deviations of the initial and final  $\phi$ -state from  $|c\rangle$ . Such deviations are model independent and generically vanish in the limit (1) as  $\sim N^{-1}$ . The following calculations for  $\phi^2\chi^2$  as well as those in subsequent sections thus represent explicit examples of the correspondence (12).

### B. Quantum calculation

There is only a single diagram (see fig. 1) entering the calculation of the rate for the process (8) at leading order in  $g^2N$ . The number of Wick contractions is canceled by the Taylor-coefficient of the relevant term of the S-matrix operator up to a factor of  $2^{n/2}$ . The diagram's multiplicity is  $n!$  and there is a factor of  $1/\sqrt{n!}$  accompanying it because of the initial  $n$ -fold occupation of the zero mode of  $\phi$ . Thus the squared amplitude is given by  $2^n n! |d|^2$ , with  $d$  the value of the diagram. If  $q_l$  denotes the virtual momentum in the propagator following the  $l$ th insertion of a pair of  $\phi$ -legs, then  $q_l^\mu = 2lm\delta_0^\mu - k^\mu$  and

the propagators contribute to  $d$  a factor of

$$\prod_{l=1}^{n/2-1} (q_l^2 - m_\chi^2)^{-1} = (-1)^{n/2-1} m^{2-n} n^2 2^{-n} (n/2)!^{-2}. \quad (13)$$

Since the initial state does not carry angular momentum, the phase space integration is trivial. Perturbatively, the kinematics are

$$nm = 2(m_\chi^2 + k^2)^{1/2}, \quad (14)$$

which corresponds to a kinematic threshold for the multiplicity  $n$  that is given by

$$n > n_0 \equiv \frac{2m_\chi}{m}. \quad (15)$$

The resulting tree-level rate for  $n\phi \rightarrow 2\chi$  is

$$\Gamma_{n\phi \rightarrow 2\chi} = \frac{1}{4\pi} V m^4 \sqrt{1 - \frac{n_0^2}{n^2}} n^4 \left( \frac{g^2}{4Vm^3} \right)^n \frac{n!}{(n/2)!^4}. \quad (16)$$

Perturbation theory can be seen not to break down regardless of the values of  $n$ . Including the combinatoric enhancement factor due to the initial  $N$  quanta,

$$C_{Nn} = \binom{N}{n} = \frac{N^n}{n!} \left( 1 + \mathcal{O}\left(\frac{n^2}{N}\right) \right), \quad (17)$$

the rate for the process (8) to leading order is given by

$$\Gamma \equiv C_{Nn} \Gamma_{n\phi \rightarrow 2\chi} \sim \left( \frac{e^2}{2n^2} \frac{g^2 \phi_0^2}{m^2} \right)^n, \quad (18)$$

where we have used relation (9), the Stirling approximation for the factorial, and omitted factors that scale less strongly with  $n$  than exponentially. The time evolution of  $n_k$ , the expected occupation number density of  $\chi$ s per momentum  $\mathbf{k}$ , is given for early times by  $n_k(t) \sim \Gamma t$ . For later times, however,  $\chi$ -Bose-enhancement becomes important, leading to an enhanced effective rate

$$\Gamma_{\text{eff}} \sim \left( 1 + 2n_k + \mathcal{O}\left(\frac{n_k^2 n^2}{N}\right) \right) \Gamma, \quad (19)$$

and thus

$$n_k(t) \sim \exp(2\Gamma t), \quad n_k \gtrsim 1. \quad (20)$$

Therefore, the connection between the quantum rate and the semiclassical prediction is provided by

$$\Gamma \sim \frac{\dot{n}_k}{n_k}. \quad (21)$$

The evolution (20) is of course neglecting modification due to sources of quantum breaking, such as depletion or evolution of entanglement. As long as the number of depleted quanta is much smaller than  $N$ , it is justified to neglect those effects.

### C. Semiclassical calculation

In the limit (10), the equations of motion simplify. The equation for  $\delta\phi$  reads

$$\begin{aligned} (\partial^2 + m^2) \delta\phi &= -2(d_t^2 + m^2) \phi_B - 2g^2 \chi^2 (\phi_B + \delta\phi) \\ &= \mathcal{O}(g). \end{aligned} \quad (22)$$

The terms involving only the background vanish due to (3). The equation for  $\chi$  reads

$$\begin{aligned} (\partial^2 + m_\chi^2) \chi &= -2g^2 \chi (\phi_B + \delta\phi)^2 \\ &= -2g^2 \phi_B^2 \chi + \mathcal{O}(g). \end{aligned} \quad (23)$$

Thus, in the limit (10),  $\delta\phi$  decouples as a free field and  $\chi$  has a time dependent contribution to its mass due to the background. For the non-perturbative solution, we can follow for example [29]. In the case of a linear equation of the form (23), the prediction for  $\chi$ -creation can be given in real time in terms of the mode function  $v_k$ , which is defined through the mode expansion of the field operator as

$$\hat{\chi}(x) = \int d^3k (v_k(t) \hat{a}_0(\mathbf{k}) e^{i\mathbf{k}\cdot\mathbf{x}} + h.c.). \quad (24)$$

Here,  $\hat{a}_0(\mathbf{k})$  and its Hermitean conjugate are the constant annihilation and creation operators. The time evolution is contained entirely in the mode function, which obeys the equation

$$(d_t^2 + \omega_k^2(t)) v_k = 0, \quad (25)$$

with

$$\omega_k^2(t) \equiv m_\chi^2 + k^2 + 2g^2 \phi_0^2 \cos^2(mt). \quad (26)$$

The expected particle-creation is then given as

$$n_k(t) \equiv \langle 0 | \hat{n}_k(t) | 0 \rangle = \frac{1}{2\omega_k} (|\dot{v}_k|^2 + \omega_k^2 |v_k|^2) - \frac{1}{2}, \quad (27)$$

where  $\hat{n}_k$  is the time evolved operator of the number density of  $\chi$ -particles per mode  $\mathbf{k}$ . The initial conditions of  $v_k$  are constrained by being consistent with the commutation relations of the operators as well as by initially defining the lowest energy state. Equations (25) and (26) imply that  $v_k$  obeys a Mathieu equation. In order to find (27) in the high multiplicity regime (11), we can refer to the treatment of the Mathieu equation in [30]. Equations (25) and (26) can be parametrized as

$$d_t^2 x + \omega_0^2 (1 + h \cos(\gamma t)) x = 0, \quad (28)$$

where the correspondence of parameters is

$$\begin{aligned} \omega_0^2 &\leftrightarrow \bar{\omega}_k^2 \equiv m_\chi^2 + k^2 + g^2 \phi_0^2, \\ h &\leftrightarrow \frac{g^2 \phi_0^2}{\bar{\omega}_k^2}, \\ \gamma &\leftrightarrow 2m. \end{aligned} \quad (29)$$

Equation (28) can exhibit so called parametric resonance, i.e., has solutions that for certain parameter combinations exhibit exponential growth between the cycles of period  $\tau \equiv 2\pi/\gamma$ :

$$x(t + \tau) = e^{s\tau} x(t), \quad (30)$$

with a parameter of instability  $s > 0$ . For the particle number one thus has

$$\frac{n_k(t + \tau)}{n_k(t)} \sim \exp(2s\tau), \quad (31)$$

and, coarse graining over several periods, one has

$$\frac{\dot{n}_k}{n_k} \sim s. \quad (32)$$

In [30], it is shown that for  $h \ll 1$ , there is parametric resonance in the bands

$$\gamma = \frac{2\omega_0}{l} + \epsilon, \quad l \in \mathbb{N}. \quad (33)$$

The maximal value of the exponent within these bands scales as

$$s \sim h^l, \quad (34)$$

as does the width  $\epsilon$ . Comparing (14) and (33), one has the correspondence  $l \leftrightarrow n/2$ . Therefore, from (21) and (32), we see that the quantum rate (18) is to be compared with  $s$  for  $2l$ :

$$s \sim h^{2l} \leftrightarrow \left( \frac{g^2 \phi_0^2}{m^2} \frac{1}{n^2} \right)^n, \quad (35)$$

where we have used (29) and  $h \ll 1$ . The agreement with the parametric scaling of (18) can be seen to be complete.

### III. EXAMPLE 2: SCALAR QED

A second example is provided by scalar QED with vanishing fundamental self-coupling of the scalar,

$$L = D_\mu \phi (D^\mu \phi)^\dagger - m^2 \phi^\dagger \phi - \frac{1}{4} F_{\mu\nu} F^{\mu\nu}, \quad (36)$$

where  $D_\mu \equiv \partial_\mu - igA_\mu$ . Let us consider the same questions as in the previous example with now  $\phi$  and  $A$  in the roles of  $\phi$  and  $\chi$ . That is, semiclassically, we consider out of the vacuum production of a photon pair in the background

$$\phi_B = \phi_B^\dagger = \phi_0 \cos(mt), \quad A_B^\mu = 0, \quad (37)$$

whereas in the fully quantum picture, we consider the many-particle annihilation processes

$$\frac{N}{2} s^- + \frac{N}{2} s^+ \rightarrow \frac{N-n}{2} s^- + \frac{N-n}{2} s^+ + 2\gamma. \quad (38)$$

quantum and classical parameters are now related by

$$\frac{N}{V} = m\phi_0^2. \quad (39)$$

and the double scaling limit (1) in semiclassical terms takes the same form as (10).

### A. Quantum calculation

The presence of the 3-point vertex,  $igA^\mu \phi^\dagger \partial_\mu \phi + h.c.$ , in principle opens up a large variety of Wick contractions contributing to the process (38) at leading order  $(Ng^2)^n$ . However, all but one of the corresponding diagrams are vanishing due to the combination of gauge redundancy and the special condensate kinematics. This can be seen as follows. All diagrams involving an incoming scalar pair connected by a single 3-point vertex vanish because the derivative yields a factor of zero in the case of the initial condensate momenta. That leaves only diagrams of the type fig. 1, where the dotted lines represent a photon and the 4-point vertices are either elementary or effective ones consisting of two 3-point vertices with one internal  $\phi$ -line:

$$-ig^2 \frac{q_{2l+2}^\mu q_{2l}^\nu}{q_{2l+1}^2 - m^2}. \quad (40)$$

Here,  $l$  is the number of vertices preceding the vertex. In every diagram with one or more vertices like (40), two momenta  $q_l$  are contracted only with photon polarization vectors that are orthogonal:

$$q_l^\mu \epsilon_\mu(q_{l'}, r) = 0, \quad \forall l, l'. \quad (41)$$

This relation holds for transverse polarizations  $r$ , which either belong to an outgoing photon or a neighbouring photon propagator, whose non-transverse part has been projected out by an outgoing photon. Thus the only non-vanishing diagram is the one constructed solely out of the elementary 4-point vertex,  $g^2 A_\mu A^\mu \phi^\dagger \phi$ . The value of the diagram is different from the 2-scalar case only by a factor

$$\epsilon_\mu^*(k, r) \epsilon^{*\mu}(k', r') = \delta_{r, r'}. \quad (42)$$

The resulting tree-level rate for  $\frac{n}{2} s^- + \frac{n}{2} s^+ \rightarrow 2\gamma$  for each of the two polarizations is thus identical with (16). The combinatoric enhancement factor due to the initial  $N$  quanta (using the Stirling approximation) is

$$C_{Nn} = \left( \frac{N/2}{n/2} \right)^2 \sim 2^{-n} \frac{N^n}{(n/2)!^2} \left( 1 + \mathcal{O}\left(\frac{n^2}{N}\right) \right). \quad (43)$$

With this and (39), the rate for the process (38) to leading order is given by

$$\Gamma \equiv C_{Nn} \Gamma_{\frac{n}{2}, \frac{n}{2} \rightarrow 2\gamma} \sim \left( \frac{e^2}{2n^2} \frac{g^2 \phi_0^2}{m^2} \right)^n, \quad (44)$$

where again we have used the Stirling approximation and omitted factors that scale less strongly with  $n$  than exponentially.

### B. Semiclassical calculation

In the limit (10), several terms in the equations of motion are suppressed. Furthermore, the background  $\phi_B$

obeys a harmonic equation and has vanishing current. Thus, with the notation

$$x \equiv \text{Re } \delta\phi, \quad y \equiv \text{Im } \delta\phi, \quad (45)$$

the equations for  $\delta\phi$  read

$$(\partial^2 + m^2)x = \mathcal{O}(g) \quad (46)$$

and

$$(\partial^2 + m^2)y = gA^\mu \partial_\mu \phi_B + g\partial_\mu (A^\mu \phi_B) + \mathcal{O}(g). \quad (47)$$

The equation for  $A_\mu$  reads

$$\partial_\mu F^{\mu\nu} = 2g^2 \phi_B^2 A^\nu - 2g(\phi_B \partial^\nu y - y \partial^\nu \phi_B) + \mathcal{O}(g). \quad (48)$$

One sees that in the limit,  $x$  decouples as a free field. Projecting out the transverse polarizations of  $A_\mu$ , their equation becomes

$$(\partial^2 - 2g^2 \phi_B^2) A_T^j = \mathcal{O}(g). \quad (49)$$

Thus, like in the previous example, the propagating photon degrees of freedom decouple from the fluctuations  $\delta\phi$ . The creation of  $s^+ s^-$  is a result of the interaction of  $y$  and the Coulomb degree of freedom encoded in  $A_0$  and  $A_L^j$ . Restricting the attention to processes of photon creation, (49) implies that the mode functions of the two transverse photon polarizations likewise obey a Mathieu equation,

$$(d_t^2 + \omega_k^2(t)) v_{k,r} = 0, \quad (50)$$

where now

$$\omega_k^2(t) \equiv k^2 + 2g^2 \phi_0^2 \cos^2(mt). \quad (51)$$

This can again be parametrized as in (28) and the analogous version of (29). Therefore, the semiclassical prediction for the rate is again

$$\frac{\dot{n}_{k,r}}{n_{k,r}} \sim \left( \frac{g^2 \phi_0^2}{m^2} \frac{1}{n^2} \right)^n. \quad (52)$$

Thus, in this example, too, the parametric agreement of (44) and (52) is complete.

#### IV. EXAMPLE 3: SCALAR QED WITH MASSIVE PHOTON

Let us consider again scalar QED, but now with a non-zero Proca mass  $m$ :

$$L = D_\mu \phi (D^\mu \phi)^\dagger - m_e^2 \phi^\dagger \phi - \frac{1}{4} F_{\mu\nu} F^{\mu\nu} + \frac{1}{2} m^2 A_\mu A^\mu. \quad (53)$$

If photon and electron in the preceding example interchange roles, we are dealing with pair-creation in an electric field. Semiclassically, we are looking at an out of the

vacuum creation of  $s^+ s^-$  in a theory with fields quantized around the background

$$A_B^\mu = \delta_z^\mu \frac{E_0}{m} \cos(mt), \quad \phi_B = 0. \quad (54)$$

The relevant processes in the fully quantum treatment on the other hand are

$$N\gamma \rightarrow (N-n)\gamma + s^+ s^-. \quad (55)$$

quantum and classical parameters are approximately related through

$$\frac{N}{V} = \frac{1}{2m} E_0^2. \quad (56)$$

The double scaling limit (1) in semiclassical terms then takes the same form as (10) with  $E_0/m$  in place of  $\phi_0$ . Equation (54) corresponds to a background electromagnetic field of the form

$$F_{0j} = \delta_j^z E_0 \sin(\omega t), \quad F_{kj} = 0, \quad (57)$$

with frequency  $\omega = m$ . This field only has an electric component pointing in  $z$ -direction. For example, it may serve as an approximate description of the field created in the antinodes of superposing laser light, on length scales short compared to the wavelength,  $2\pi/\omega$ . For an optical or X-ray laser, the kinematic threshold is necessarily high,  $n_0 \equiv 2m_e/m \gg 1$ . This is in contrast to the previous examples with  $m_\chi$  arbitrary and  $m_\gamma = 0$ , respectively. For such a hierarchy, the dominant process is the one closest to the threshold,

$$n = n_0 + \delta, \quad 0 < \delta \leq 1, \quad (58)$$

as follows from the scaling of (18) and (44) and will turn out to be the case here, too. The regime (11) for  $n \sim n_0$  corresponds to

$$\frac{gE_0}{mm_e} \ll 1. \quad (59)$$

#### A. Semiclassical result

The semiclassical rate of pair-creation in the background field (57) averaged over a period of oscillation has been found in [31, 32] (see also [33]) in the regime of  $n_0 \gg 1$  and  $E_0 \ll m_e^2/g$ . The full result interpolates between the following two asymptotic expressions. In the regime of  $\frac{gE_0}{m_e\omega} \gg 1$ , the rate asymptotes to

$$\Gamma \sim \frac{Vm_e^4}{2\sqrt{2}\pi^4} \left( \frac{gE_0}{m_e^2} \right)^{5/2} \exp\left(-\pi \frac{m_e^2}{gE_0}\right), \quad (60)$$

which is essentially the suppression obtained by Schwinger for the case of a constant electric field [34].

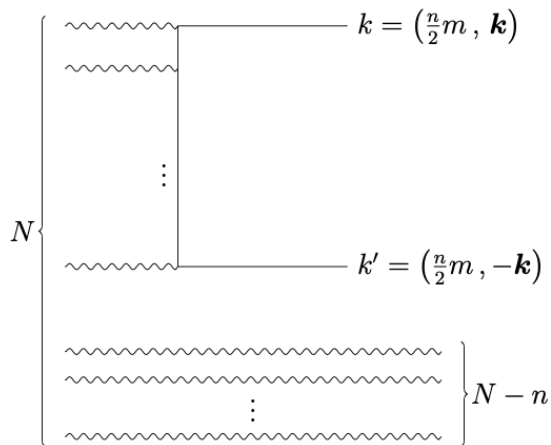


FIG. 2. One of the terms contributing to the amplitude of the process (55).

For the opposite case,  $\frac{gE_0}{m_e\omega} \ll 1$ , the result is asymptotic to

$$\Gamma \sim \frac{Vm_e^4}{(2\pi)^{5/2}} e^{-2\delta} \left(\frac{\omega}{m_e}\right)^{5/2} \left(\frac{e g E_0}{4 m_e \omega}\right)^{2(n_0+\delta)} \text{Erfi}(\sqrt{2\delta}). \quad (61)$$

The latter regime is sometimes referred to as the multi-photon regime and coincides with (59). In the following perturbative quantum calculation, we indeed fully reproduce (61) in terms of an  $n$ -photon process (55).

## B. Quantum calculation

In the present case, all possible Wick contractions lead to non-vanishing diagrams. However, near the kinematic threshold, one particular diagram dominates over the others. This is the diagram constructed purely out of the 4-point vertex, as obtained from the digram in fig. 1 upon exchanging  $\phi$ s for  $\gamma$ s and the  $\chi$ -pair for  $s^+s^-$ . Let us denote by  $\delta\Gamma_4$  the contribution to the rate from the square of only that diagram. Isolating such contributions may be useful despite the contribution of interference terms in the case in which certain diagrams dominate over others. In terms of the rate (16) in the 2-scalar example, we have

$$\delta\Gamma_4 = 2^{-n-1}\Gamma_{n\phi\rightarrow 2\chi}. \quad (62)$$

Here, the relative factor of  $2^{-n}$  comes from the lesser number of Wick contractions since the complex field  $\phi$  replaces the real field  $\chi$ . Likewise, there is another relative factor of  $1/2$ , since the final particles are not identical. All other diagrams feature photon-insertions via 3-point vertices. The opposite extreme case of the diagram considered above, arising from contracting solely 3-point vertices, is depicted in fig. 2. Let us denote by  $\delta\Gamma_3$  the contribution based on its square. It can be obtained in

an analogous calculation and the result is

$$\frac{\delta\Gamma_3}{\delta\Gamma_4} = \frac{e^{2n}}{8n} \left(1 - \frac{n_0^2}{n^2}\right)^n \sim \frac{e^{2n}}{8n} \left(\frac{2\delta}{n_0}\right)^n, \quad (63)$$

where the last relation holds for the dominant process (58). This is strongly suppressed for sufficiently small  $\delta/n_0$ . The above consideration indicates that a 3-point vertex results in a suppression factor near the threshold and that therefore for the process (58) the amplitude is well approximated by the diagram in fig. 1. We thus have

$$\Gamma_{n\gamma\rightarrow s^+s^-} = \delta\Gamma_4 (1 + \mathcal{O}(\delta)). \quad (64)$$

The combinatoric enhancement is the same as in (17). Relating  $N$  and  $E_0$  via (56), we thus have

$$\Gamma \sim \frac{1}{8\pi^3} Vm^4 \sqrt{1 - \frac{n_0^2}{n^2}} n^2 \left(\frac{e g E_0}{4 m_e m n}\right)^{2n}, \quad (65)$$

where we have used (17) and the Stirling approximation. For the process (58), one has  $1 - (n_0/n)^2 \sim 2\delta/n_0$  as well as  $(n_0/n)^{2n} \approx e^{-2\delta}$ . Using these relations, (65) can be seen to agree completely with (61), if in the latter one retains only the leading order of

$$\text{Erfi}(\sqrt{2\delta}) = 2\sqrt{\frac{2}{\pi}}\sqrt{\delta} \left(1 + \frac{2}{3}\delta + \mathcal{O}(\delta^2)\right). \quad (66)$$

The relative error for  $\delta \ll 1$  is thus  $\sim \delta$  and for  $\delta = 1$  it is  $\approx 0.6$ .

## V. PARAMETER REGIMES

In the preceding sections, we have considered the rate for a many particle process of the form  $n \rightarrow 2$  in the example of three different models. In a certain regime, we have found a result which scales  $\sim (g^2 N)^n$ . In this section, we are going to look in more detail at the limits of validity of this leading order approximation. For definiteness, we are going to base the discussion on the  $\phi^2\chi^2$ -model.

### A. Semiclassical limit

In the limit (1), the following two things happen. First, the backreaction from the created  $\chi$ -quanta on the state of  $\phi$  vanishes. Secondly, loop corrections, that are higher order in  $g^2$ , vanish as well.

As a result, any non-perturbative treatment that exploits a semiclassical approximation and neglects radiative corrections becomes exact. Of such kind are the semiclassical calculations referenced in the three examples considered.

Their result can be understood as the resummation of the set of diagrams that do not vanish in the limit (1). Those diagrams are of the same order in  $N$  and in  $g^2$ .

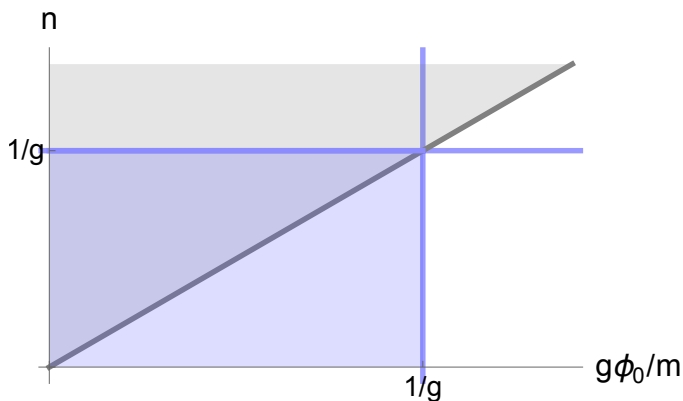


FIG. 3. Schematic representation of regime boundaries: Above the grey diagonal line, non-perturbative corrections are negligible (see (67)). Additional regimes for finite  $g^2$  (and the example of negligible  $m_\chi$ ): To the left of the blue vertical line, loop corrections to the potential are negligible (see (69)); Below the blue horizontal line, contributions of loop induced diagrams are negligible (see (74)). The overlap of coloured areas is the resulting regime in which the calculation is perturbative in both  $g^2N$  and  $g^2$ , i.e., both non-perturbative and quantum corrections to the leading order approximation are negligible.

At the leading order,  $n$ , those are the diagrams that we evaluated in the quantum perturbative calculations. At higher orders,  $n+k$ , those are what may be called forward scattering diagrams, with  $k$   $\phi$ -quanta all scattered into the initial mode.

As we have seen, in the regime (11) (regime (59), respectively), which in terms of  $N$  reads

$$n^2 \gg \frac{g^2 N}{Vm^3}, \quad (67)$$

the diagrams beyond the leading order,  $k \geq 1$ , are negligible. On the other hand, when approaching the opposite regime, the effect of their resummation is both to shift the kinematic threshold through an effective contribution to the particle masses and to alter the scaling of the rate. The power-law growth with coupling and field strength gets softened before the rate becomes large. In the case of the Mathieu analysis (in sec.s II and III), that is the transition between narrow and broad resonance. For the example of pair-creation in the alternating electric field (sec. IV), the interpolation is shown in (60) and (61).

Fig. 3 offers a schematic graphical representation of the perturbative and non-perturbative regime in the parameter plane of  $n$  and  $g\phi_0/m$  as well as further regimes to be discussed below.

### B. Finite $g^2$

For finite  $N$  and  $g^2$ , there are various quantum corrections arising.

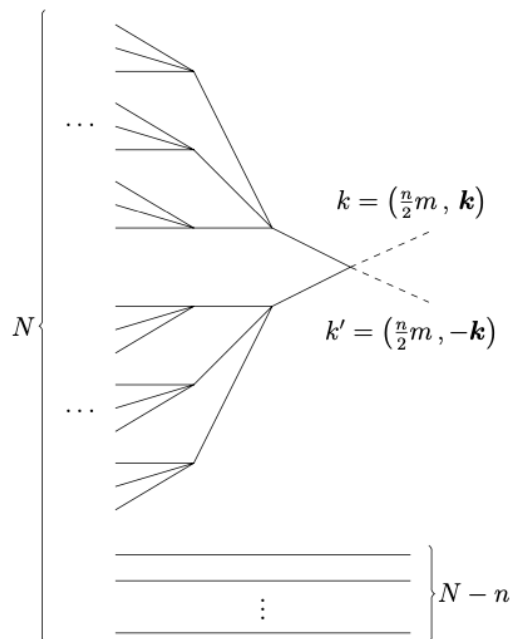


FIG. 4. "Symmetrically branching tree" (SBT) diagram: Diagram contributing to the amplitude of the process  $n\phi \rightarrow 2\chi$  based on only a single cross coupling vertex and otherwise only the quartic self-coupling of  $\phi$  (with the most symmetric shape possible).

Corrections of backreaction-type, such as depletion or evolution of entanglement, are  $1/N$ -suppressed [5, 10]. Although such corrections build up over time, for the first emissions they are negligible in the case of sufficiently large  $N$ .

Likewise, corrections due to a single loop or contributions from processes with a single (non-forward) scattered  $\phi$  are negligible due to the extra power of the coupling  $g^2$ .

In the following we attempt to identify and estimate other loop effects that may be significant despite  $g^2 \ll 1$ . For simplicity, from now on we are going to focus on the case of a negligible mass  $m_\chi$ .

#### 1. Effective potential

Consider the effective potential at 1-loop [35]. For  $\chi = 0$ ,  $\phi$  moves in the potential

$$V_{1Loop}(\phi, 0) = \frac{m^2}{2}\phi^2 + \frac{g^4\phi^4}{16\pi^2} \left( \log\left(\frac{2g^2\phi^2}{\mu^2}\right) - \frac{3}{2} \right), \quad (68)$$

where parameters are defined in  $\overline{\text{MS}}$ . For  $\phi$ -values for which the loop-correction is not negligible, the time evolution  $\phi(t)$  as in (3) as well as the energetics relating  $N$  and  $\phi_0$  as in (9) are altered and the considerations of the preceding sections do not go through. Equation (68) implies that quantum corrections of this kind are only

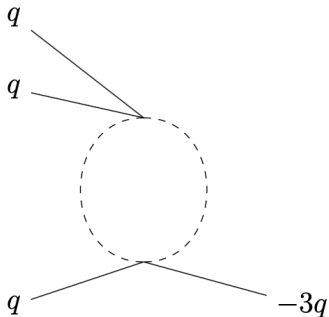


FIG. 5. Momentum dependent 4- $\phi$ -vertex induced by a  $\chi$ -loop with momenta as occurring in the SBT diagram (fig. 4)

negligible for (with a choice of  $\mu \sim m$ )

$$\frac{\phi_0}{m} \ll \frac{1}{g^2}. \quad (69)$$

This constrains the initial state in terms of the theory parameter  $g^2$  (see fig. 3).

## 2. Diagrams with different $n$ -scaling

Another kind of quantum correction may come from loop diagrams that compared to the leading order are suppressed by much higher powers of  $g^2$ , but on the other hand feature a significantly different scaling with  $n$ . This may happen due to different momentum flow through a diagram permitted by different Wick contractions. In particular, a quartic self-coupling of  $\phi$  gives rise to a well-known case of a diagram with strong  $n$ -scaling [36, 37]. This is the "symmetrically branching tree" (SBT) diagram shown in fig. 4.

The required self-coupling is induced via the cross-coupling through a  $\chi$ -loop (see fig. 5) and the corresponding momentum dependent vertex has the value

$$v_4(q^2) = -\frac{ig^4}{16\pi^2} \left( \log\left(\frac{4q^2}{\mu^2}\right) - 2 + i\pi \right) + \mathcal{O}(g^6). \quad (70)$$

As is evident from figs 4 and 5, we have  $m^2 \leq q^2 \leq \frac{1}{9}n^2m^2$ , depending on the position of the vertex in the diagram. Therefore, there is no significant  $n$ -scaling implicit in the momentum dependence of the vertex and  $4!|v_4| \sim g^4$  serves as a good estimate throughout the diagram.

The rate based on only the square of the SBT diagram can be found in a calculation analogous to the ones given in [36, 37]. For the present purposes, the following schematic representation is sufficient:

$$\delta\Gamma_{SBT} \sim \left(\frac{c}{Vm^3}\right)^n n!, \quad c \sim g^4. \quad (71)$$

Due to the presence of the factorial, perturbation theory breaks down for

$$n \gtrsim n_{max} \equiv \frac{Vm^3}{c}. \quad (72)$$

Comparing the contribution (71) with the leading order rate (16), we see that it becomes important for

$$n \gtrsim n_{eq} \equiv \sqrt{g^2/c}, \quad (73)$$

which takes place well before the breakdown. There are of course further diagrams as well as interference, but we may take (73) as an indication for the  $n$ -regime where contributions due to loop-induced couplings are no longer negligible. The limit of validity of the leading order approximation (16) is then parametrically given by

$$n \ll \frac{1}{g}, \quad (74)$$

which is a bound independent of the initial state parameter  $\phi_0$ .

As can be seen in fig. 3, the combination of constraints on  $\phi_0$  (on  $N$ ) and  $n$  leaves a finite area in which corrections due to effects of higher order in  $g^2$  and in  $g^2N$  are negligible.

## VI. QUANTUMIZATION AND CLASSICALIZATION

It is an outstanding question under what conditions a classical system can reach a regime in which the classical approximation is no longer applicable and how rapidly this can happen. In this respect, the first important concept, introduced within the black hole  $N$ -portrait [1], was *macro-quantumness* [4, 38]. This term encoded the previous observations that  $1/N$  quantum effects lead to features that cannot be accounted classically, e.g., emergence of black hole hair [3].

The question about the speed of the breakdown of classicality was posed in [2] (and extended in [5, 8]), where this phenomenon was called "quantum breaking" and the corresponding timescale the "quantum break-time",  $t_Q$ .

In [2] it was shown that in an  $N$ -particle system that exhibits a Lyapunov instability, the quantum break-time can be logarithmically short,

$$t_Q = \lambda^{-1} \ln(N), \quad (75)$$

where  $\lambda$  is the Lyapunov exponent. In particular, this effect was explicitly demonstrated for the 1+1-dimensional condensate of bosons on a ring with attractive interaction [2] (for a more recent discussion of this model, see [39]).

On the other hand, for a system that exhibits no classical instability, the situation is different. For such a system the following general bound on the quantum break-time was imposed [8]:

$$t_Q \sim \frac{N}{N^2\Gamma_{2 \rightarrow 2}}. \quad (76)$$

Here,  $\Gamma_{2\rightarrow 2}$  is the re-scattering rate of a pair of constituents. We deliberately kept the  $\sim N^2$  factor in the denominator, which comes from the Bose-enhancement of the initial quanta. Basically, it counts the number of pairs in the condensate, which is  $C_{Nn} = N(N-1)/2$ . The expression (76) says that in order for the condensate to quantum break, of order  $N$  scattering acts must take place. For the example of a self-coupled scalar of [8], the expression (76) has been reproduced in [15] via different methods.

In other words, the main engine for quantum breaking is a gradual loss of coherence due to scattering of small number of constituents into the external quanta, as opposed to non-gradual, i.e., single-process transitions with the participation of many constituents. For a stable classical system, single-process transitions into a quantum state are suppressed.

To this type of processes, in the present paper, we give the special name of *quantumization*. Although the term can be defined in a broader sense, the processes that we have studied here, specifically amount to transitions from an initially classical state into a quantum state with a small number of constituents. Such processes can be viewed as the transitions from macro to micro systems.

The opposite process, a single-process transition from a few-particle quantum state into a classical one, is known as classicalization [21–26].

Our analysis contributes into understanding of physics of both processes and in their very different manifestations.

In particular while unsuppressed classicalization is possible in certain systems, quantumization is universally suppressed. At first glance, this may sound rather surprising, since both processes originate from the same basic phenomenon: transition from few to many, or vice versa. For definiteness, under “few” let us think of two-particle state  $|2\rangle$  and under “many” the state  $|n\rangle$  of  $n \gg 1$  quanta. We shall assume that both are approximated as valid asymptotic  $S$ -matrix states.

The basic ingredient controlling both transition processes is the square of the  $S$ -matrix element  $|\langle 2 | \hat{S} | n \rangle|^2$ . This element is always suppressed. In fact using very general arguments based on the effective Hamiltonian and locality of the Hilbert space, one can argue that at weak coupling and large  $n$  this element is bounded from above (cf. [26], which refines [25]),

$$|\langle 2 | \hat{S} | n \rangle|^2 \leq e^{-n}. \quad (77)$$

However, in the estimate of the total probability of the transition, the matrix element is summed over the degeneracy of the final states [1],

$$\Gamma_{i\rightarrow f} \propto \sum_f |\langle 2 | \hat{S} | n \rangle|^2. \quad (78)$$

Depending on whether the out state is  $\langle 2 |$  or  $\langle n |$ , the degeneracy factors can be dramatically different. In particular, the degeneracy of two-particle states can never

be exponentially large, without compromising the validity of the theory, whereas the degeneracy of  $n$ -particle states can [26]. This is the core reason for why quantumization and classicalization are realised in nature very differently.

We shall discuss the two phenomena separately and compare them. For definiteness, in the following, we are going to refer to the  $\phi^2\chi^2$ -example. The discussion equally applies to the other examples.

### A. Quantumization

The bound (76) provides an explanation of the fact that quantumization phenomena are commonly not observed. For example, telecommunication does not suffer from complications due to transitions of electromagnetic waves to mostly quantum states upon encountering a charged particle. Neither is quantumization expected for objects that are not directly observed. To repeat the example given in the introduction, a black hole is not expected to decay into a pair of high energetic photons although no conservation law would bar such a transition.

The systems studied above allow us to observe the reason for suppression explicitly. In the considered systems, quantumization would correspond to the process  $n \rightarrow 2$  with  $n \sim N$ . In this case, an order one fraction of the energy stored in the initial coherent state is transferred to the created particle pair.

Since the basic  $S$ -matrix element is suppressed, the rate requires enhancement due to combinatorics associated with either initial or the final states or both.

One possibility is the enhancement due to large number of choices of  $n$  quanta from the total set of initial particles.

However, we must note that the increase of the initial occupation number of quanta up to a level  $N \sim g^{-4}$ , will invalidate the weak coupling treatment. Firstly, in such a regime, the collective interaction from the rest, substantially modifies the dispersion relation of each particle. Secondly, for such a high occupation number, the condensate develops Lyapunov instabilities and a coherently oscillating field (3) no longer represents a valid classical background. This is also clear from the one-loop effective potential (68), which corrects the free oscillations for amplitudes exceeding  $m/g^2$ . Correspondingly, the validity of our treatment is limited by (69), which in terms of  $N$  reads

$$N \ll \frac{Vm^3}{g^4}. \quad (79)$$

To make the above explicit in the example of a condensate decaying into a particle pair, let us compare the predicted decay time to the timescale of an oscillation,  $\sim m^{-1}$ , or to the one required for a complete gradual decay,

$$\tau_{gradual} \lesssim N \Gamma_{2\rightarrow 2}^{-1} \sim m^{-1} N \frac{Vm^3}{g^4}. \quad (80)$$

This upper bound is neglecting the Bose-enhancement due to the  $N$  quanta in the initial state (which is taken into account in (76)) as well as the accumulating Bose-enhancement due to the created  $\chi$ -particles (corresponding to the occurrence of parametric resonance in the Mathieu-equation (25)). We shall see that nevertheless non-gradual decay is negligible during timescales on the order of (80).

The coherent superposition is sharply peaked around the mean occupation  $N$ , but it has non-zero support for other occupations, including ones higher than  $N$ . In order to parametrize the range of  $n$  corresponding to  $n \sim N$  we may therefore introduce a parameter  $r$  and sum the rates for processes with  $N/r \leq n \leq rN$  (where appropriate rounding is implicit and values  $r \gtrsim 10$  are sensible). This range of  $n$  is in the perturbative regime (67) as long as

$$r^2 \ll NVm^3/g^2. \quad (81)$$

Depending on the number state in the coherent superposition, for a given  $n$ , there is a number  $n'$  of unscattered initial quanta. The sum over final states therefore includes a sum over  $n'$ . To see what effective combinatoric enhancement that sum amounts to for a given  $n$ , we note that

$$\begin{aligned} \sum_{n'=0}^{\infty} |\langle n' | \hat{a}^n | c \rangle|^2 &= \sum_{n'=0}^{\infty} \binom{n+n'}{n} |\langle 0 | \hat{a}^n | n \rangle \langle n+n' | c \rangle|^2 = \\ &= \frac{N^n}{n!} |\langle 0 | \hat{a}^n | n \rangle|^2, \end{aligned} \quad (82)$$

where the occupations of the number states such as  $|n\rangle$  and of the coherent state  $|c\rangle$  are all referring to the same mode and  $\hat{a}|c\rangle = \sqrt{N}|c\rangle$ . We therefore have for the rate of non-gradual decay

$$\Gamma_{n \sim N} \sim \sum_{n=N/r}^{rN} \frac{N^n}{n!} \Gamma_{n \rightarrow 2}. \quad (83)$$

In the regime where for the quantity  $\Gamma_{n \rightarrow 2}$  the result (16) is valid, we see that the timescale  $\Gamma_{n \sim N}^{-1}$  is much larger than (80), as long as (81) is fulfilled. If instead the scaling (71) is valid, the summation range of  $n$  is within the perturbative unitarity bound (72) if  $N \leq n_{max}/f$ , which coincides with (79). In that case we see that  $\Gamma_{n \sim N}^{-1}$  is still much larger than (80).

Likewise, the rate of quantumization cannot be enhanced significantly through degeneracy of the final 2-particle states. The reason is that the exponential increase of 2-particle degeneracy would make the theory strongly coupled, thereby invalidating the degrees of freedom.

A simple way for illustrating this is to notice that the degeneracy of final states can be increased by endowing the  $\chi$ -particles with an internal ‘‘flavor’’ quantum number  $j = 1, 2, \dots, N_f$ . For example,  $\chi_j$  can form an  $N_f$ -dimensional representation of the  $SO(N_f)$  symmetry

group. This of course will increase the rate (16) of the transition  $n\phi \rightarrow 2\chi$  by a factor  $N_f$ . However,  $N_f$  cannot be arbitrarily large. The requirement that  $\phi$  and  $\chi$ -particles be valid (weakly interacting) degrees of freedom, puts the following bound on the collective coupling:

$$N_f g^4 \lesssim 1. \quad (84)$$

Violation of this bound changes the regime of the theory. In particular this is signalled by the breakdown of the loop expansion.

The above bound makes the enhancement of the quantumization process negligible as compared to the exponential suppression of the matrix element (77).

Notice that the suppression of a fast transition from the classical state of  $n$   $\phi$ s into a quantum state of two  $\chi$ s also illustrates the difficulty of rapid generation of quantum entanglement from the classical state. Indeed, the  $SO(N_f)$ -invariant 2-particle state,

$$|2\rangle = \frac{1}{\sqrt{N_f}} \sum_{j=1}^{N_f} |\chi_j\rangle \times |\chi_j\rangle, \quad (85)$$

is entangled with respect to the flavor quantum number. However, its production rate is highly suppressed. Instead in a classically stable system the entanglement can only be generated gradually and requires the time of order (76) [5, 6, 11].

## B. Classicalization

The story is very different for classicalization processes [21]. Such a process comes from the inverse transition  $2 \rightarrow n$  [22, 24–26].

Of course, for a fixed pair of initial and final states, the absolute values of  $S$ -matrix elements for transitions in both directions,  $|S_{2 \rightarrow n}|$  and  $|S_{n \rightarrow 2}|$ , are exactly equal. However, the degeneracy of an  $n$ -particle final state is potentially much higher. If the degeneracy is sufficiently high, it can overcome the suppression. This is the essence of classicalization [25, 26].

For example, endowing  $\phi_j$  with the  $SO(N_f)$  index, exponentially increases the degeneracy of the available states with  $n$   $\phi$ -bosons [26]. Of course, by symmetry, the transition elements to each member of the same irreducible representation are equal. The end-result is enhanced by the dimensionality of the representation. For example, a symmetric state of  $n$  quanta has degeneracy  $C_{N_f+n,n} = (N_f+n)!/n!N_f!$ , which scales as  $e^n$  for  $N_f \sim n$ . Of course, we do not claim that a simple  $\phi^2\chi^2$ -theory exhibits classicalization at order-one rate, but the tendency of enhancement of classicalizing transition  $2 \rightarrow n$  versus quantumization process  $n \rightarrow 2$  is clear.  
1

<sup>1</sup> Notice that one could try to enhance the rate of an  $n \rightarrow 2$  quantum-

Correspondingly, the  $n$ -particle states of high entropy, the so-called saturons, can in principle be produced with unsuppressed rate in a collision of two energetic quanta [26]. Nature provides an example of a saturon in the form of black holes.

It has been believed for a long time [40–42] that a black hole can form in a collision of two particles with unsuppressed probability. This view is supported by the semiclassical intuition that a black hole must form whenever energy is localized within its gravitational radius. In particular, this feature served as the basis for the idea of self-completion of gravity [43].

However, as usual, without a microscopic theory of a black hole, it is impossible to verify and understand the underlying quantum mechanism for its unsuppressed formation. This is provided by the black hole  $N$ -portrait [1], where a black hole is described as a condensate of  $N$  soft gravitons, with the microstate entropy  $\sim N$ .

In this theory, the creation of a black hole from colliding quanta represents an instance of classicalization,  $2 \rightarrow N$ , in which a highly degenerate  $N$ -graviton state is formed [1]. Due to the high multiplicity involved in the process, the probability of transition to each microstate is suppressed by  $e^{-N}$  [24, 27]. Despite this, the total probability of black hole formation is of order one. The reason for this is found in the non-perturbative enhancement of the transition rate due to degeneracy of the  $N$ -graviton state, which accounts for the black hole entropy [1, 24].

The high multiplicity nature of a black hole likewise serves as an explanation of stability against instantaneous decay. Indeed, such a decay,  $N \rightarrow 2$ , is controlled by the same exponentially suppressed  $S$ -matrix element as the formation process,  $N \rightarrow 2$  [1, 24]. However, the crucial difference from the formation case is the lack of the entropy-enhancement. This is due to an insufficient degeneracy of the final 2-particle state. This explains why a classical black hole cannot explode into two (or few) particles.

Of course, the term “explosion into few particles” in the case of a black hole must be taken with a grain of salt, since the decay products gravitate. Correspondingly, if the particles materialize at separations not much larger than the initial gravitational radius, the accompanying classical gravitational field is too strong to be neglected. Calculationwise, this merely amounts to a dressing of the outgoing energetic quanta with a classical gravitational

field in the form of a coherent state of secondary “softer” gravitons.

It has been suggested [44] that another candidate for the saturated entropy state is a Color Glass Condensate of gluons in QCD [45]. The formation of this state in collision of protons can then be viewed as a process of classicalization. It has also been proposed [26] that confinement in QCD with large number of colors can be interpreted as the process of formation of a saturated state of gluons due to excessive color degeneracy.

The formation of saturon bound states in a  $2 \rightarrow N$  process within the Gross-Neveu model [46] has been studied in [47]. This analysis clearly indicates the entropy enhancement of an otherwise exponentially suppressed transition rate.

## VII. SUMMARY AND OUTLOOK

In the present paper we have resolved a class of non-perturbative semiclassical phenomena in terms of perturbative quantum processes involving many quanta. This continues the line previously applied to objects such as black holes [1] and de Sitter [1, 5] (see section I for a more complete list of references). This resolution makes certain properties very transparent. One very important physical implication is the universal suppression of *quantumization*, defined as a single-process transition from a classical object to a few-particle quantum state.

Classically stable objects, such as coherently oscillating fields, black holes, or de Sitter space do not “explode” via creation of few highly energetic quanta. Rather they lose coherence gradually, via quantum processes that involve scattering of a small number of constituents. Likewise, entanglement cannot be generated via a single-process transition but requires a gradual development.

The fundamental effect unifying all these seemingly distinct systems is the suppression of many-particle  $S$ -matrix elements describing  $N \rightarrow 2$  (or  $N \rightarrow \text{few}$ ) transitions between basic number eigenstates. Previously, this has been argued to be the case in  $2 \rightarrow N$  graviton scattering [1] and explicitly verified in [24]. The suppression of  $2 \rightarrow N$  matrix-elements has also been argued on very general grounds in [26].

The present study reduces the phenomenon to its bare essentials and explicitly traces its origin within the most elementary quantum field theories. Specifically, we have explicitly demonstrated the effect within the simplest interacting scalar and gauge theories.

Our analysis is directly extendable to the case of particle-creation in an oscillating background spin-2 field, which, in particular, has been used as a resolution of de Sitter space [5].

We have shown that in the large- $N$  double-scaling limit (1), the perturbative quantum results fully match the semiclassical computations, which usually are considered to be non-perturbative in nature.

At the same time, our analysis helps to visualize why

---

mization process by taking the initial  $n$ -particle state as the normalized invariant integral over the entire representation space. This would enhance the amplitude by the dimensionality of the representation. However, such an initial state represents a superposition of all basis state vectors and cannot be regarded as classical. Therefore, such a transition does not fall in our category of quantumization processes. However, such transitions can potentially play an important role in the evolution of a macroscopic system, such as a black hole, after its quantum break-time, since by then the system can evolve into an entangled superposition of many microstates (see the discussion in VII).

the phenomenon of classicalization, based on the inverse transition  $\text{few} \rightarrow N$ , may be unsuppressed if the  $N$ -particle state has a sufficient microstate degeneracy [26].

In particular, this is the case for black holes [1]. The microstate degeneracy does not assist the process of quantumization if the initial state of the object is described by one particular microstate. Such absence of superposition is a necessary condition of classicality.

It is important that the classicality of a state is distinguished from its macroscopic nature. After  $t_Q$  the system, e.g., a black hole, continues to be macroscopic but it is no longer classical. Due to this, past the half-decay time all bets are off.

For example, after  $t_Q$ , dramatic modifications in black hole evolution can take place. In particular, as shown in [6], the backreaction from the stored quantum information (the so-called “memory burden” effect [48]) becomes overwhelming and the Hawking-approximation breaks down fully.

Past this point, the following two pathways were outlined in [6]. One, as indicated by simulations of prototype systems, is the slowdown of the initially dominant gradual decay process. This, however, does not exclude

the development of a new classical instability and correspondingly the appearance of a Lyapunov exponent leading to the disintegration of the black hole [6]. Then, in the light of [2] and of the present discussion, this can serve as a trigger of unsuppressed quantum processes. That is, at the level of present understanding, past its half decay, we cannot exclude a further explosive evolution of a black hole, neither quantum nor classical.

## ACKNOWLEDGMENTS

It is a pleasure to thank Max Warkentin for conversations.

The figures of diagrams have been created using *TikZ-Feynman* [49].

This work was supported in part by the Humboldt Foundation under Humboldt Professorship Award, by the Deutsche Forschungsgemeinschaft (DFG, German Research Foundation) under Germany’s Excellence Strategy - EXC-2111 - 390814868, and Germany’s Excellence Strategy under Excellence Cluster Origins.

- 
- [1] G. Dvali and C. Gomez, Black Hole’s Quantum N-Portrait, *Fortsch. Phys.* **61**, 742 (2013), arXiv:1112.3359 [hep-th]; Black Holes as Critical Point of Quantum Phase Transition, *Eur. Phys. J.* **C74**, 2752 (2014), arXiv:1207.4059 [hep-th].
  - [2] G. Dvali, D. Flassig, C. Gomez, A. Pritzel, and N. Wintergerst, Scrambling in the Black Hole Portrait, *Phys. Rev.* **D88**, 124041 (2013), arXiv:1307.3458 [hep-th].
  - [3] G. Dvali and C. Gomez, Black Hole’s 1/N Hair, *Phys. Lett.* **B719**, 419 (2013), arXiv:1203.6575 [hep-th].
  - [4] G. Dvali and C. Gomez, Black Hole Macro-Quantumness, (2012), arXiv:1212.0765 [hep-th].
  - [5] G. Dvali and C. Gomez, Quantum Compositeness of Gravity: Black Holes, AdS and Inflation, *JCAP* **1401**, 023, arXiv:1312.4795 [hep-th].
  - [6] G. Dvali, L. Eisemann, M. Michel, and S. Zell, Black hole metamorphosis and stabilization by memory burden, *Phys. Rev. D* **102**, 103523 (2020), arXiv:2006.00011 [hep-th].
  - [7] G. Dvali and C. Gomez, Quantum Exclusion of Positive Cosmological Constant?, *Annalen Phys.* **528**, 68 (2016), arXiv:1412.8077 [hep-th].
  - [8] G. Dvali, C. Gomez, and S. Zell, Quantum Break-Time of de Sitter, *JCAP* **1706**, 028, arXiv:1701.08776 [hep-th].
  - [9] G. Dvali, L. Eisemann, M. Michel, and S. Zell, Universe’s Primordial Quantum Memories, *JCAP* **1903**, 010, arXiv:1812.08749 [hep-th].
  - [10] G. Dvali,  $S$ -Matrix and Anomaly of de Sitter, *Symmetry* **13**, 3 (2020), arXiv:2012.02133 [hep-th].
  - [11] G. Dvali, Quantum gravity in species regime, (2021), arXiv:2103.15668 [hep-th].
  - [12] L. Berezhiani, G. Dvali, and O. Sakhelashvili, de Sitter space as a BRST invariant coherent state of gravitons, *Phys. Rev. D* **105**, 025022 (2022), arXiv:2111.12022 [hep-th].
  - [13] G. W. Gibbons and S. W. Hawking, Cosmological Event Horizons, Thermodynamics, and Particle Creation, *Phys. Rev.* **D15**, 2738 (1977).
  - [14] G. Dvali and S. Zell, Classicality and Quantum Break-Time for Cosmic Axions, *JCAP* **07**, 064, arXiv:1710.00835 [hep-ph].
  - [15] L. Berezhiani and M. Zantedeschi, Evolution of coherent states as quantum counterpart of classical dynamics, *Phys. Rev. D* **104**, 085007 (2021), arXiv:2011.11229 [hep-th].
  - [16] L. Berezhiani, G. Cintia, and M. Zantedeschi, Background-field method and initial-time singularity for coherent states, *Phys. Rev. D* **105**, 045003 (2022), arXiv:2108.13235 [hep-th].
  - [17] F. Kühnel, Thoughts on the Vacuum Energy in the Quantum N-Portrait, *Mod. Phys. Lett. A* **30**, 1550197 (2015), arXiv:1408.5897 [gr-qc].
  - [18] F. Kühnel and M. Sandstad, Corpuscular Consideration of Eternal Inflation, *Eur. Phys. J. C* **75**, 505 (2015), arXiv:1504.02377 [gr-qc].
  - [19] L. Berezhiani, On Corpuscular Theory of Inflation, *Eur. Phys. J. C* **77**, 106 (2017), arXiv:1610.08433 [hep-th].
  - [20] L. Kofman, A. D. Linde, and A. A. Starobinsky, Towards the theory of reheating after inflation, *Phys. Rev. D* **56**, 3258 (1997), arXiv:hep-ph/9704452.
  - [21] G. Dvali, G. F. Giudice, C. Gomez, and A. Kehagias, UV-Completion by Classicalization, *JHEP* **08**, 108, arXiv:1010.1415 [hep-ph].
  - [22] G. Dvali, C. Gomez, and A. Kehagias, Classicalization of Gravitons and Goldstones, *JHEP* **11**, 070, arXiv:1103.5963 [hep-th].
  - [23] G. Dvali, Strong Coupling and Classicalization, *Subnucl. Ser.* **53**, 189 (2017), arXiv:1607.07422 [hep-th].

- [24] G. Dvali, C. Gomez, R. S. Isermann, D. Lüüst, and S. Stieberger, Black hole formation and classicalization in ultra-Planckian  $2 \rightarrow N$  scattering, *Nucl. Phys. B* **893**, 187 (2015), arXiv:1409.7405 [hep-th].
- [25] G. Dvali, Classicalization Clearly: Quantum Transition into States of Maximal Memory Storage Capacity, (2018), arXiv:1804.06154 [hep-th].
- [26] G. Dvali, Entropy Bound and Unitarity of Scattering Amplitudes, *JHEP* **03**, 126, arXiv:2003.05546 [hep-th].
- [27] A. Addazi, M. Bianchi, and G. Veneziano, Glimpses of black hole formation/evaporation in highly inelastic, ultra-planckian string collisions, *JHEP* **02**, 111, arXiv:1611.03643 [hep-th].
- [28] T. W. B. Kibble, Frequency Shift in High-Intensity Compton Scattering, *Phys. Rev.* **138**, B740 (1965).
- [29] N. D. Birrell and P. C. W. Davies, *Quantum Fields in Curved Space*, Cambridge Monographs on Mathematical Physics (Cambridge Univ. Press, Cambridge, UK, 1984); V. Mukhanov and S. Winitzki, *Introduction to quantum effects in gravity* (Cambridge University Press, 2007).
- [30] L. Landau and S. Lifshitz, E., *Mechanics, Vol.1, pp. 80-84* (Butterworth-Heinemann, 1976).
- [31] M. S. Marinov and V. S. Popov, Electron-Positron Pair Creation from Vacuum Induced by Variable Electric Field, *Fortsch. Phys.* **25**, 373 (1977).
- [32] E. Brezin and C. Itzykson, Pair production in vacuum by an alternating field, *Phys. Rev. D* **2**, 1191 (1970).
- [33] A. Ringwald, Pair production from vacuum at the focus of an X-ray free electron laser, *Phys. Lett. B* **510**, 107 (2001), arXiv:hep-ph/0103185.
- [34] J. S. Schwinger, On gauge invariance and vacuum polarization, *Phys. Rev.* **82**, 664 (1951).
- [35] S. R. Coleman and E. J. Weinberg, Radiative Corrections as the Origin of Spontaneous Symmetry Breaking, *Phys. Rev. D* **7**, 1888 (1973).
- [36] H. Goldberg, Breakdown of perturbation theory at tree level in theories with scalars, *Phys. Lett. B* **246**, 445 (1990).
- [37] J. M. Cornwall, On the High-energy Behavior of Weakly Coupled Gauge Theories, *Phys. Lett. B* **243**, 271 (1990).
- [38] D. Flassig, A. Pritzel, and N. Wintergerst, Black holes and quantumness on macroscopic scales, *Phys. Rev. D* **87**, 084007 (2013), arXiv:1212.3344 [hep-th].
- [39] A. Kovtun and M. Zantedeschi, Breaking BEC, *JHEP* **07**, 212, arXiv:2003.10283 [hep-th].
- [40] G. 't Hooft, Graviton Dominance in Ultrahigh-Energy Scattering, *Phys. Lett. B* **198**, 61 (1987).
- [41] D. Amati, M. Ciafaloni, and G. Veneziano, Superstring Collisions at Planckian Energies, *Phys. Lett. B* **197**, 81 (1987); Classical and Quantum Gravity Effects from Planckian Energy Superstring Collisions, *Int. J. Mod. Phys. A* **3**, 1615 (1988).
- [42] D. J. Gross and P. F. Mende, String Theory Beyond the Planck Scale, *Nucl. Phys. B* **303**, 407 (1988); The High-Energy Behavior of String Scattering Amplitudes, *Phys. Lett. B* **197**, 129 (1987).
- [43] G. Dvali and C. Gomez, Self-Completeness of Einstein Gravity, (2010), arXiv:1005.3497 [hep-th].
- [44] G. Dvali and R. Venugopalan, Classicalization and unitarization of wee partons in QCD and gravity: The CGC-black hole correspondence, *Phys. Rev. D* **105**, 056026 (2022), arXiv:2106.11989 [hep-th].
- [45] F. Gelis, E. Iancu, J. Jalilian-Marian, and R. Venugopalan, The Color Glass Condensate, *Ann. Rev. Nucl. Part. Sci.* **60**, 463 (2010), arXiv:1002.0333 [hep-ph].
- [46] D. J. Gross and A. Neveu, Dynamical Symmetry Breaking in Asymptotically Free Field Theories, *Phys. Rev. D* **10**, 3235 (1974).
- [47] G. Dvali and O. Sakhelashvili, Black-hole-like saturons in Gross-Neveu, *Phys. Rev. D* **105**, 065014 (2022), arXiv:2111.03620 [hep-th].
- [48] G. Dvali, A Microscopic Model of Holography: Survival by the Burden of Memory, (2018), arXiv:1810.02336 [hep-th].
- [49] J. Ellis, TikZ-Feynman: Feynman diagrams with TikZ, *Comput. Phys. Commun.* **210**, 103 (2017), arXiv:1601.05437 [hep-ph].